

ARTICLE

OPEN



Effect of TGF- β mediated phenotypic changes on prostate cancer cell anoikis response

Prerna R. Nepali ¹, Edgar Gonzalez-Kozlova ^{2,3}, Maitri Anegondi ⁴, Navneet Dogra ^{3,5}, Maddison Archer ¹, Goutam Chakraborty ^{1,6}, Ashutosh K. Tewari ¹, Benjamin D. Hopkins ⁴ and Natasha Kyprianou ^{1,2,5}

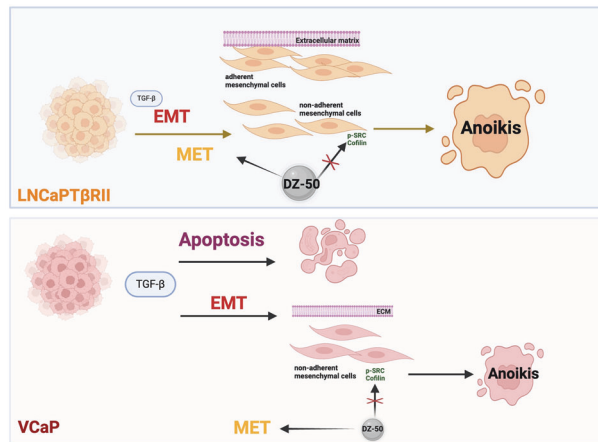
© The Author(s) 2025

Epithelial mesenchymal transition (EMT) circumvents anoikis (cell death upon detachment from extracellular matrix) to promote prostate metastasis and therapy resistance. In this study, we investigated how TGF- β regulated EMT-MET (mesenchymal epithelial transition) phenotypic interconversions to enhance anoikis response in pre-clinical models of prostate cancer (PCa). We used human PCa cell line models: VCaP (androgen-sensitive, TGF- β responsive); 22RV1 (castration resistant prostate cancer); LNCaP; LNCaPT β RII (LNCaP cells overexpressing TGF- β receptor II, androgen-sensitive, TGF- β responsive); C4-2B parental and C4-2B TaxR (TGF- β unresponsive, taxane resistant). We assessed their response to TGF- β (EMT inducer) and two antitumor agents (DZ-50 and cabazitaxel (CBZ)) to understand the effect of EMT priming on anoikis vulnerability. Our findings demonstrate: (1) TGF- β induces EMT in LNCaPT β RII and apoptosis in VCaP. (2) LNCaPT β RII cells are primed by EMT to anoikis (downregulation of pSRC and cofilin). (3) Metabolic changes occur at EMT-anoikis intersection in LNCaPT β RII. (4) DZ-50 overcomes CBZ resistance in C4-2B TaxR and improves response in cells and castration-resistant organoids. These studies indicate that prostate cancer cells "programmed" to undergo phenotypic EMT become vulnerable to cell death via anoikis. Exploitation of this intersection is of potential significance in overcoming resistance to taxane chemotherapy in lethal prostate cancer.

Oncogene (2025) 44:4835–4845; <https://doi.org/10.1038/s41388-025-03600-z>

Graphical Abstract

The intersection between EMT and anoikis in prostate cancer cells. TGF- β responsive prostate cancer cells respond differentially to TGF- β by undergoing epithelial mesenchymal transition EMT (LNCaPT β RII and VCaP) or apoptosis (VCaP). TGF- β induced EMT further sensitizes LNCaPT β RII to DZ-50 induced anoikis. DZ-50-associated anoikis cell death in prostate cancer cells is associated with (i) phenotypic reprogramming (EMT to mesenchymal epithelial transition (MET)) (ii) inactivation of SRC (decreased pSRC) (iii) decreased cofilin expression in LNCaPT β RII and VCaP cells.



¹Department of Urology, Icahn School of Medicine at Mount Sinai, New York, NY, USA. ²Department of Immunology and Immunotherapy, Icahn School of Medicine at Mount Sinai, New York, NY, USA. ³Department of Genomic Sciences, Icahn School of Medicine at Mount Sinai, New York, NY, USA. ⁴The Engleander Institute for Precision Medicine, Weill Cornell Medicine, New York, NY, USA. ⁵Department of Pathology and Molecular & Cell Based Medicine, Icahn School of Medicine at Mount Sinai, New York, NY, USA. ⁶Department of Oncological Sciences, Icahn School of Medicine at Mount Sinai, New York, NY, USA. email: Natasha.Kyprianou@mountsinai.org

Received: 1 May 2025 Revised: 12 September 2025 Accepted: 6 October 2025
Published online: 22 November 2025

INTRODUCTION

There is a severe gap in knowledge in the development of targeted therapeutics to overcome prostate tumor recurrence and progression towards lethality. The challenges with prostate cancer management are a result of resistance to treatment modalities of androgen-deprivation therapy (ADT), radiotherapy and chemotherapy [1, 2]. As androgen receptor (AR) signaling is one of the major drivers of prostate cancer growth, ADT has been the predominant standard of care approach; however, the initial response is followed by the emergence of castration-resistant prostate cancer (CRPC) [1, 3]. This advanced metastatic CRPC (mCRPC) can be therapeutically targeted with AR signaling inhibitors, such as Abiraterone Acetate and Enzalutamide [4, 5]. After the emergence of resistance to ADT and AR inhibitors, patients are treated with 1st line (Docetaxel), 2nd line taxane chemotherapy cabazitaxel (CBZ) or with the recently approved by the FDA, DNA-damaging agents, such as poly ADP-Ribose Polymerase Inhibitors [4, 6–9].

Tumor cell death via apoptosis is the hallmark response to cancer treatment, and defects in the apoptotic machinery are associated with cancer progression, metastasis, and therapeutic resistance [1, 10, 11]. Anoikis is apoptosis induced upon disruption of cell-extracellular matrix interactions (ECM) [1, 12]. Cancer cells develop mechanisms to escape anoikis and survive independent of ECM interactions during epithelial-mesenchymal transition (EMT) and metastatic spread [1, 13]. Previous studies in our lab via structural optimization of doxazosin have led to a novel lead quinazoline-based derivative DZ-50, which has shown therapeutic promise through its properties to impair tumor growth and metastatic invasion by overcoming anoikis resistance [14–16]. In human androgen-independent prostate cancer cells (PC-3 and DU-145), DZ-50 has shown anti-tumor benefits by causing structural disruption of focal adhesions (fibronectin, integrin- $\alpha 6$ and talin) and tight junctions (claudin-11) [15]. DZ-50 also influences the phenotypic reprogramming of human prostate cancer cells [EMT to mesenchymal epithelial transition (MET)] by targeting insulin-like growth factor binding protein-3 as seen via increased expression of the epithelial marker E-cadherin and decreased mesenchymal marker N-cadherin in human prostate cancer cell lines [17]. Moreover, we have demonstrated that DZ-50 enhances the anti-tumor response of therapeutically resistant prostate cancer to the anti-androgen enzalutamide [16]. Phenotypic reprogramming and the resultant prostate tumor cell vulnerability to anoikis are potentially dependent on autocrine and/or paracrine TGF- β signaling from the tumor microenvironment. Cofilin, an F-actin severing protein that is essential for cytoskeletal reorganization, is also involved in enhancing cell migration and invasiveness of prostate cancer cells in response to TGF- β [18].

Our previous studies demonstrated that treatment with CBZ (2nd line taxane chemotherapy) contributes to the phenotypic reprogramming (EMT to MET) of prostate cancer cells [19]. In this study, we leveraged TGF- β as an EMT inducer and the novel compound DZ-50 as a pharmacologic tool to induce anoikis, in order to determine the impact of EMT-anoikis intersection on overcoming prostate tumor therapeutic resistance.

MATERIALS AND METHODS

Cell lines

Human prostate cancer cell lines 22RV1 (CRPC) (CRL-2505) (RRID:CVCL_1045) and LNCaP (androgen sensitive) (CRL-1740) (RRID:CVCL_1379) were obtained from ATCC, Manassas, VA. Therapeutically resistant human prostate cancer cell lines (C4-2B parental and C4-2B TaxR-TGF β unresponsive, taxane resistant) were generously provided by Dr. Allen Gao (University of California, Davis) [20, 21] (C4-2B parental: RRID: CVCL_4784, C4-2B TaxR: developed in Gao lab by culturing C4-2B cells in docetaxel in a dose-escalation manner). The LNCaP cells overexpressing

the TGF- β receptor II (LNCaPT β RII-androgen-sensitive; TGF- β responsive) have been established in our laboratory [17, 22]. These cells were maintained in RPMI medium (10-040CM) from Corning, NY, supplemented with 10% Fetal Bovine Serum and 1% Penicillin-Streptomycin from Thermo Fisher Scientific, MA, in an incubator (37 °C, 5% CO₂). VCaP cells (androgen-sensitive; TGF- β responsive) (ATCC CRL-2876) (RRID:CVCL_2235) were cultured in Dulbecco's Modified Eagle's Medium containing 4500 mg/L glucose (30-2002) from ATCC, Manassas, VA supplemented with 10% Fetal Bovine Serum and 1% Penicillin-Streptomycin.

Drugs and chemicals

The therapeutic agent DZ-50 was developed in our lab [14]. CBZ (Sigma Aldrich) was dissolved to 1 mM stock in 100% ethanol. Recombinant Human TGF-1 beta Protein (TGF- β) (240-B-010 from R&D Systems, MN) was reconstituted to 100 µg/mL in sterile 4 mM HCl containing 1 mg/mL bovine serum albumin. Galunisertib (LY2157299) (S2230 from Selleck Chemicals) was diluted to 5 mM stock in dimethyl sulfoxide (DMSO). Dasatinib (S1021) was obtained from Selleck Chemicals.

Cell viability assay

Cell viability was assessed using the Thiazolyl Blue Tetrazolium bromide (MTT) assay. Cells were grown to 60–75% confluence in a 96-well plate and treated with DZ-50 in the presence or absence of 5 ng/ml TGF- β for 4 h pre-treatment. The impact of TGFBR inhibition on TGF- β induced EMT and DZ-50 induced cell death was assessed using 10 µM Galunisertib. Dasatinib (0.3 µM) alone or in combination with DZ-50 (2 or 5 µM) was used to inhibit SRC and measure the impact on cell viability over a time course (24, 48, 72 or 96 h). To study whether the therapeutic response of prostate cancer cells to CBZ can be improved by co-administration with DZ-50, a time course of 24, 48, 72 or 96 h was conducted by treating cells with CBZ alone (10 nM), DZ-50 (2 or 5 µM) alone or CBZ with DZ-50. Cells were subsequently treated with MTT (M6494 from Thermo Fisher Scientific, MA) for 1 h at 37 °C and formazan crystals were solubilized with DMSO. Absorbance was measured at 570 nm using a SpectraMax M5 spectrophotometer (Molecular Devices, CA). Results are represented as Mean ± SEM of three independent experiments.

Western blotting

Whole cell lysates from cells subjected to differential treatments were collected using RIPA lysis buffer (89900) supplemented with protease and phosphatase inhibitor (A32961) from Thermo Fisher Scientific, MA. Protein concentration was measured using the BCA Protein Assay Kit. SDS-polyacrylamide gel electrophoresis was performed using 12% Precast polyacrylamide Protein Gels (4561044 from BioRad, CA). Proteins were transferred to PVDF membranes, and membranes were exposed to primary antibody (4 °C, overnight incubation) and secondary antibody. Primary and secondary antibodies were purchased from Cell Signaling, MA, except Zeb1 (Bethyl Labs, Fortis Life Sciences, TX), Smad4 (Abcam, MA), and GAPDH (Santa Cruz Biotechnology, TX). Protein bands were detected by enhanced chemiluminescence using the SuperSignal West Femto Maximum Sensitivity substrate (Thermo Fisher Scientific, MA) and visualized using Amersham ImageQuant 800. Some membranes were subjected to mild stripping using Restore Western Blot Stripping Buffer (Thermo Fisher Scientific, MA) and reprobed.

Matrigel invasion assay

The BioCoat Matrigel Invasion Chamber with Matrigel Matrix (Thermo Fisher Scientific, MA) was used for this assay, and the chambers and wells were pre-incubated with serum-free media for 2 h. Cell suspension in serum-free media was seeded in the chambers, and the bottom wells were filled with FBS-containing culture medium. After incubation for 48 h, non-invasive cells were scrubbed off with a medium-moistened cotton swab. The cells at the lower surface of the chambers were then stained with the Diff-Quick staining solutions (IMEB Inc., San Marcos, CA). Images were captured at $\times 10$ magnification, and the number of invading cells was counted in 4 fields (from three independent experiments).

Anoikis evaluation

Six-well plates were coated with poly(2-hydroxyethylmethacrylate) (Poly-HEMA) (Sigma Aldrich) and allowed to dry. Cells were seeded onto polyHEMA coated plates and treated for 24 h with 5 ng/ml TGF- β or 5 µM DZ-50. Untreated cells were used as controls [23]. Twenty-four hours after

treatment, cells were harvested from polyHEMA-coated wells with trypsin/EDTA to yield a single cell suspension. The numbers of viable and dead cells were determined by trypan blue and counting on an automated Countess cell counter (Thermo Fisher Scientific, MA) [24].

RNA seq-transcriptomic analysis

RNA isolation and RNA-seq of LNCaPT β RII and VCaP cells was performed at the Center for Advanced Genomics Technology at Icahn School of Medicine at Mount Sinai. We used 50 bp single-end and 50 million reads per sample for a total of four treatment conditions for each cell line (untreated, 5 ng/ml TGF- β 24 h, 5 μ M DZ-50 for 9 h or 5 ng/ml TGF- β pre-treatment followed by 5 μ M DZ-50 for 9 h). Each treatment condition was performed in triplicates. Illumina Stranded mRNA library prep kit was used to prepare the RNA material for sequencing. NovaSeq SP FlowCell 300 cycles V1.5 was utilized to amplify the mRNAs. Briefly, the resulting reads were quality controlled using FASTQC, Multi-QC and SamTools. The reads were aligned to Human Genomic Reference HG38 with splicing sensitive aligner STAR 2.7. Gene counts were quantified using FeatureCounts. Downstream differential expression analysis and pathway enrichment were performed using R packages Dream, mle4, Variance Partition, enrichR, GSVA and figures were generated with ggplot2, tidyverse, complex heatmap and pheatmap packages. Data is available upon request and under the SRA folder.

Organoid viability assessment [25]

CRPC organoids [26] were plated in triplicate in 5 μ L dots with 1000 cells/microliter in (1:2 media to Matrigel) each well of a 96-well plate. These plates were left for five days for organoids to form and expand before dosing. Organoids were then treated with six doses of drugs at indicated concentrations. DMSO (0.1%) treated cells were used as a control. After 72 h of treatment cell viability was assessed using Cell-Titer Glo 3D cell viability assay (Promega), which measures ATP levels within the cells. The average luminescence of the control wells normalize the drug treated wells. Drug response curves were generated for each drug using the PRISM 10 software.

Statistical analysis

Data are shown as means \pm standard error of mean (SEM). Statistical analysis was performed using GraphPad Prism 9 software and R/R Studio. Comparisons of single treatments were done using Student's *t* test and multi group comparisons were performed with one-way ANOVA followed by Tukey's post hoc test or Dunnett's multiple comparisons test to determine the significance between groups. Multiple treatments within groups were assessed with repeated-measures ANOVA followed by Newman-Keuls or Tukey's post hoc test. Significance was at $p < 0.05$. Transcriptomic analyses were normalized by library size using the R package edgeR, limma, variance Partition and Dream. Differential expression analysis used moderate t-tests and mixed effect models to control for false discovery rate. Adjusted $p < 0.05$ was considered statistically significant.

RESULTS

TGF- β induces a differential response in prostate cancer cells
TGF- β is a multifunctional cytokine that serves as a growth inhibitor and apoptosis inducer in early-stage prostate tumor growth and as a metastasis promoter during tumor progression [27]. We first examined the response of two TGF- β -responsive human prostate cancer cell lines, LNCaPT β RII and VCaP to TGF- β . The LNCaPT β RII cells do not undergo cell death in response to TGF- β (Fig. 1a). This observation correlated with transcriptional downregulation of hallmark apoptotic genes in LNCaPT β RII cells after TGF- β exposure compared to untreated cells (Fig. 1b). In VCaP cells, TGF- β induced an apoptotic response as revealed by the significant loss of cell viability (in a time dependent manner) (Fig. 1c). Transcriptomic analysis showed an upregulation of the hallmark apoptosis genes in VCaP post TGF- β treatment (Fig. 1d). We further investigated the individual gene expression in the apoptosis pathway revealing significant ($FDR < 0.05$) deregulation between the cell lines (with TGF- β , DZ-50 or combination of TGF- β and DZ-50) (Fig. 1e, f). Each cell line exhibited a distinct profile of

gene expression in response to TGF- β with differential deregulation of apoptotic genes (Fig. 1e, f). Treatment with DZ-50, alone or post-TGF- β exposure, reverses gene expression profile by down-regulating genes previously upregulated by TGF- β in LNCaPT β RII cells (e.g., SPCAN1, RHOT2, BCL2L11, CDKN1A, and NEDD9) (Fig. 1e).

Collectively, the transcriptomic analysis showed increased expression of apoptosis genes in VCaP cells post TGF- β treatment (Fig. 1f), and that NEDD9 is significantly upregulated in LNCaPT β RII cells in response to TGF- β . Furthermore, DZ-50 and TGF- β with DZ-50 increased JAM2 gene expression in LNCaPT β RII cells, implicating metabolic deregulation.

Prostate cancer cell response to anoikis-induction is primed by TGF- β mediated EMT

We subsequently investigated whether the TGF- β -induced differential response in prostate cancer cells can be leveraged for therapeutic advantage in prostate tumors: (a) which respond to TGF- β via EMT to induce cell death by anoikis, and (b) which respond to TGF- β by undergoing apoptosis to initiate further cell death by anoikis. To determine the functional contribution of TGF- β in linking EMT with anoikis, we blocked TGF- β activity with galunisertib [TGF- β receptor I (T β RI) inhibitor] and assessed the impact on cell viability. As observed in Fig. 1, TGF- β alone does not impact survival of LNCaPT β RII cells, but DZ-50 is able to significantly decrease cell viability compared to untreated controls (Fig. 2a). Interestingly after pre-treatment of LNCaPT β RII cells with TGF- β (24 h), DZ-50 can further decrease cell viability (55.26% with DZ-50 5 μ M or 32.40% with DZ-50 10 μ M) (Fig. 2a). In the presence of a combination of galunisertib (10 μ M) and TGF- β (5 ng/ml, 24 h pre-treatment), DZ-50 (at varying concentrations) can reduce cell viability of LNCaPT β RII cells to 70% which is comparable to DZ-50 alone (Fig. 2a). The VCaP cells exhibited significant cell death in a dose response manner to DZ-50 monotherapy (2, 3, 4, 5, 10 μ M). In contrast to the LNCaPT β RII cells, the apoptotic response of VCaP to DZ-50 is not affected by TGF- β pre-treatment, nor was there a consequential effect of EMT on these cells (Fig. 2b). TGF- β alone acts as an inducer of cell death in VCaP cells (Fig. 1c), pre-treatment with a combination of TGF- β and galunisertib did not impact cell death induced by DZ-50 in VCaP cells (Fig. 2b).

Analysis of the transcriptomic profile that TGF- β induced significant changes in gene expression in LNCaPT β RII cells treated with DZ-50 (Fig. 2c). The major differences in the principal component (PC) of VCaP cells were consequential to DZ-50 treatment with or without TGF- β prior exposure to (Fig. 2d). The VCaP cells showed upregulation ($FDR < 0.05$) of unique pathways, such as transmembrane receptor signaling activity, G-protein coupled receptor, lipase and phospholipase activities (Supplementary Fig. 1). In LNCaPT β RII cells there was an upregulation of intracellular remodeling and metabolism associated pathways, such as nucleic acid binding and organelle/intracellular membrane regulation. Post TGF- β treatment, both cell lines underwent profound transcriptomic changes, however, key differences between the cell lines were sustained (Fig. 2e, f). Pathway enrichment analysis revealed increased cytoskeleton remodeling in VCaP, while LNCaPT β RII showed a novel set of metabolic and differentiation signals, including increased L-serine and steroid dehydrogenase activity (Fig. 2f).

These results indicate that prostate cancer cells undergo a differential response to TGF- β , apoptosis and EMT or EMT induction alone.

Anoikis induction leads to phenotypic changes in prostate cancer cells

TGF- β elicits diverse responses in different human prostate cancer cells, such as apoptosis in VCaP cells but not in LNCaPT β RII. To gain mechanistic insights into the induction of EMT by TGF- β and the ability of DZ-50 to interject with phenotypic reprogramming

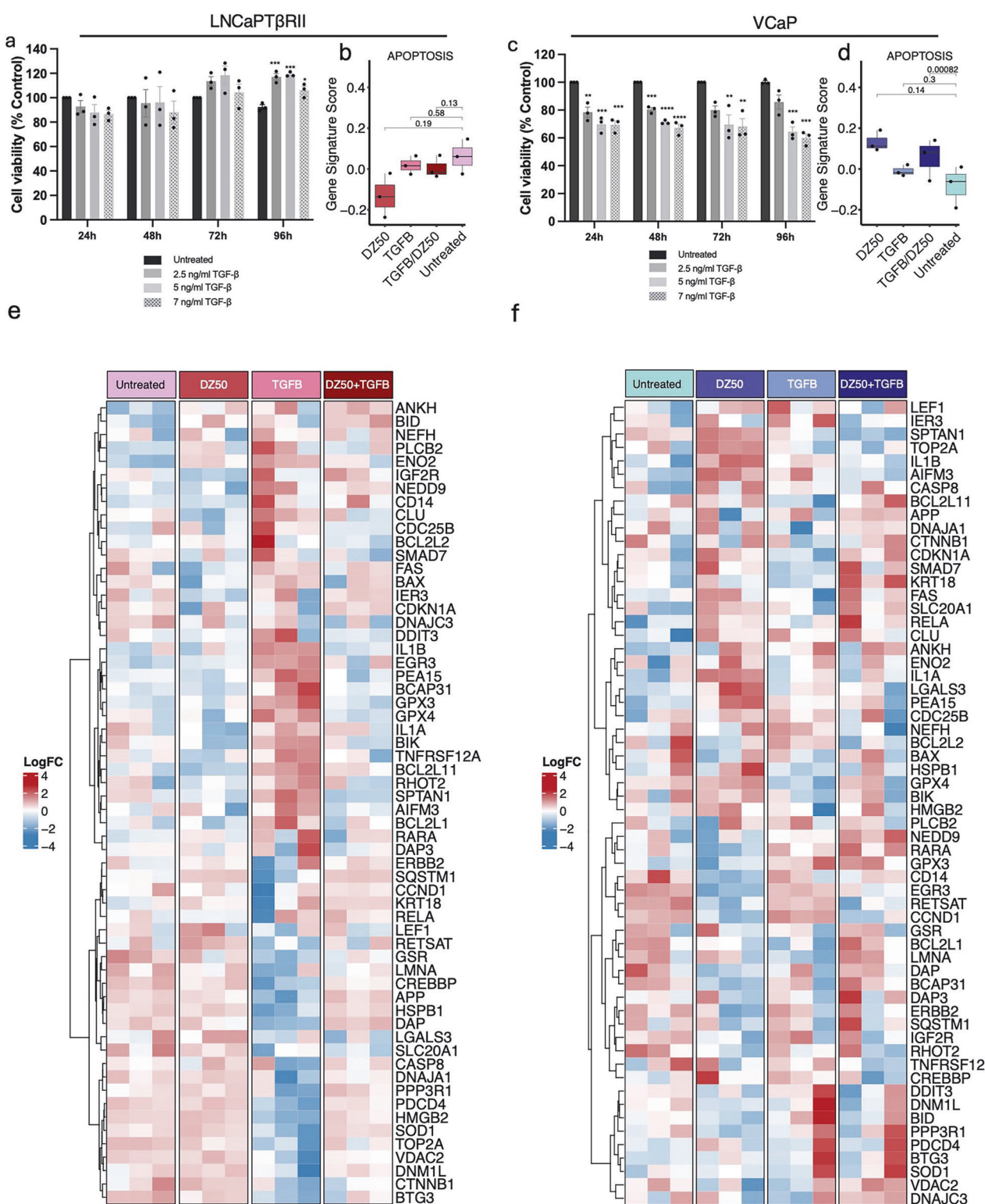


Fig. 1 TGF- β stimulation induces cell death in VCaP cells. **a** LNCaPT β RII cells do not undergo apoptosis in response to different concentrations of TGF- β stimulation over a time-course as assessed by MTT assay. **b** The hallmark RNA gene signature for apoptosis in LNCaPT β RII cells showed downregulation for every treatment, yet the strongest effect was observed in DZ-50 alone. **c** Cell viability of VCaP cells as measured by MTT assay is reduced in response to TGF- β (2.5 ng/ml, 5 ng/ml or 7 ng/ml concentration treated for 24, 48, 72 or 96 h). **d** The hallmark apoptotic gene signature in VCaP cells shows an increase in response to DZ-50, TGF- β or combination compared to untreated controls. (Error bars \pm SEM. ** p < 0.01, *** p < 0.001, **** p < 0.0001. n = 3 independent experiments, each done in triplicates). **e, f** The individual genes which are part of the hallmark pathway for apoptosis are shown for both cell lines. Approximately half of the genes show downregulation and the other half shows upregulation. A paired t-test was used to compare the gene signatures, and the genes showed in the heatmap are significant in at least 1 statistical comparison using mixed effect models and differential expression analysis.

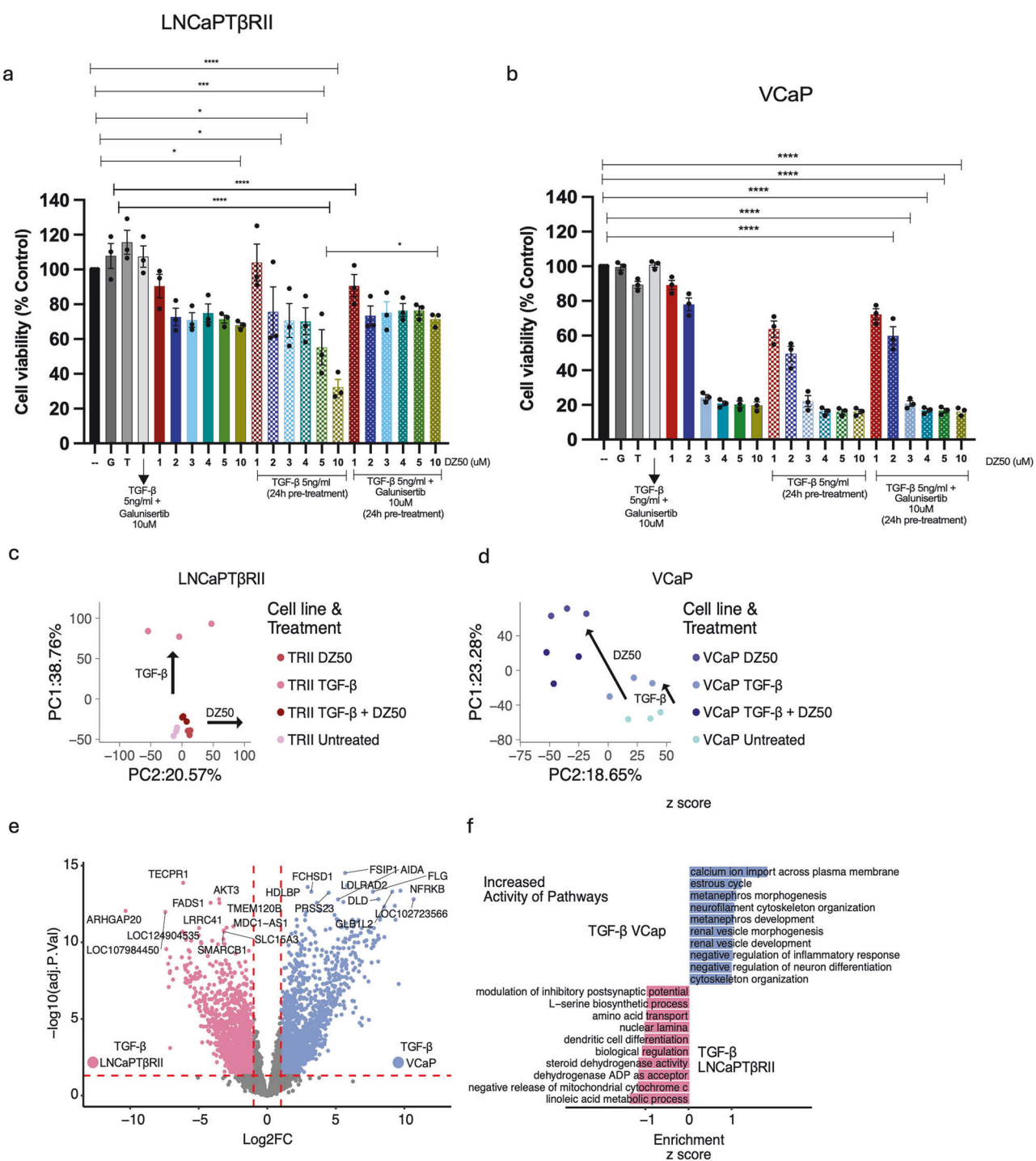


Fig. 2 Anoikis response is improved in TGF- β treated LNCaPT β RII cells. Cell viability assay in **a** LNCaPT β RII cells or **b** VCaP cells in response to DZ-50 alone or with 24 h of TGF- β pre-treatment (5 ng/ml) or with 24 h TGF- β pre-treatment and Galunisertib (10 μM). Controls include untreated cells, galunisertib alone (G), TGF- β alone (T) and TGF- β + Galunisertib. TGF- β pre-treatment improved the response of LNCaPT β RII cells to DZ-50 induced cell death. Bars \pm SEM $n=3$ independent experiments. Each experiment was performed in triplicates. * $p < 0.05$, ** $p < 0.01$, *** $p < 0.001$, **** $p < 0.0001$. **c, d** represent the principal component (PC) of the transcriptomic landscape in **c** LNCaPT β RII cells and **d** VCaP cells. **e** Volcano plots representing changes in genes in LNCaPT β RII cells (pink) and VCaP cells (blue) after TGF- β treatment. **f** Top enriched gene pathways in LNCaPT β RII cells compared with VCaP (blue) and in VCaP cells compared with LNCaPT β RII (pink).

(EMT-MET), we examined the protein expression profile of EMT effectors in response to TGF- β (EMT inducer), DZ-50 (anoikis inducer) for 24 or 48 h or DZ-50 after the cells are pre-treated with TGF- β . To explore the functional contribution of TGF- β signaling in determining phenotypic outcomes prior to anoikis, we subsequently used galunisertib, the T β RI receptor inhibitor. In

LNCaPT β RII cells, DZ-50 alone did not change the expression of epithelial or mesenchymal markers (Fig. 3a). In a similar pattern wherein the TGF- β and DZ-50 combination improved the therapeutic response of LNCaPT β RII cells (Fig. 2a), DZ-50 reduced the expression of vimentin and snail (24 and 48 h) only after TGF- β pre-treatment (Fig. 3a). Snail expression in LNCaPT β RII cells was

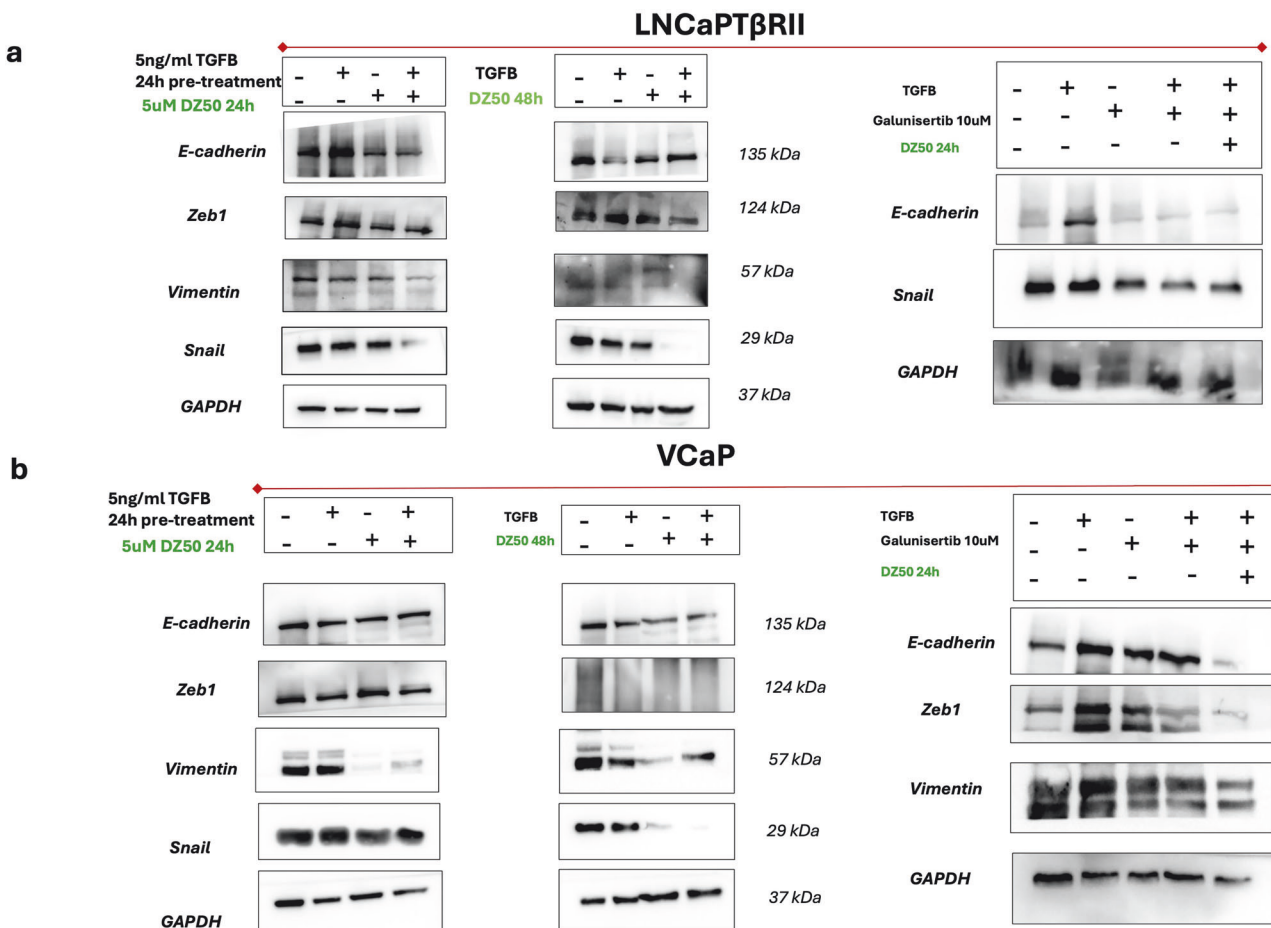


Fig. 3 Anoikis induction by DZ-50 decreases mesenchymal markers in prostate cancer cells. Protein expression of EMT markers in **a** LNCaPT β RII cells and **b** VCaP cells after: (i) no treatment, (ii) TGF- β (5 ng/ml), (iii) DZ-50 (5 μ M, 24 or 48 h) or (iv) 24 h pre-treatment with TGF- β followed by DZ-50 (5 μ M, 24 or 48 h). The blots on the right side represent EMT markers in **a** LNCaPT β RII cells and **b** VCaP cells receiving (i) no treatment (ii) Galunisertib (10 μ M) (iii) DZ-50 (5 μ M, 24 or 48 h) (iv) TGF- β (5 ng/ml) and Galunisertib (10 μ M) (v) 24 h pre-treatment with TGF- β and Galunisertib followed by DZ-50 (5 μ M, 24 or 48 h). The data represents three independent experiments. Mesenchymal markers (vimentin and snail) were decreased in prostate cancer cell lines after DZ-50 treatment.

also markedly reduced upon TGF- β and galunisertib exposure followed by DZ-50 (Fig. 3a).

In VCaP cells, DZ-50 reduced vimentin and snail protein levels after 48 h (Fig. 3b). We pre-treated VCaP with EMT/ apoptotic inducer TGF- β (5 ng/ml, 24 h) and observed that TGF- β led to a decrease in E-cadherin (24 and 48 h) and DZ-50 was able to reverse this effect and downregulate protein expression of vimentin and Snail indicating that anoikis induction led to phenotypic reversal (mesenchymal to epithelial) (Fig. 3b). RNAseq analysis also shows a significant decrease in the Snail gene after DZ-50 treatment in VCaP cells but not in vimentin (Supplementary Fig. 2).

TGF- β -responsive prostate cancer cells exhibit anoikis vulnerability

Activated (phosphorylated) Src (p-SRC) confers anoikis resistance and is associated with poor clinical outcomes in prostate cancer [23, 28]. To investigate the mechanism of DZ-50 induced prostate cancer cell death we treated LNCaPT β RII and VCaP cells with DZ-50 and assessed the protein expression of p-SRC. Along with the cell death induced by DZ-50 (Fig. 2), DZ-50 treatment decreases p-SRC in both LNCaPT β RII (post 48 h) and VCaP cells (post 24 and 48 h) (Fig. 4a, b). After EMT priming of the cells via TGF- β pre-treatment (5 ng/ml for 24 h) we observed reduction in p-SRC protein levels in both cell types after DZ-50 (Fig. 4a, b). The LNCaPT β RII cells exhibited sensitivity to DZ-50 after they were

primed with TGF- β as shown by reduced phosphorylation of SRC (Figs. 2a and 4a).

Pre-treatment with galunisertib and TGF- β followed by DZ-50 (5 μ M) led to a decrease in pSRC in LNCaPT β RII cells (Fig. 4a). The caspase-induced cleavage of Poly ADP-ribose polymerase-1 (PARP-1) is a classic marker of apoptosis [29], and PARP-1 has also been shown to be a regulator of Smad-dependent responses of TGF- β signaling directing them toward EMT in prostate cancer progression [30]. We detected PARP cleavage after treatment of LNCaPT β RII cells with DZ-50 alone or TGF- β prior to DZ-50 for 48 h, indicating apoptotic induction by DZ-50 even after triggering TGF- β signaling/EMT in these cells (Fig. 4a). PARP cleavage was also observed in VCaP cells after DZ-50 alone or in combination with TGF- β (Fig. 4b). There was an increase in the TGF- β signaling effector Smad-4 protein levels in response to TGF- β , DZ-50 or TGF- β + DZ-50 in LNCaPT β RII cells. Smad 4 protein expression was increased in VCaP cells after 48 h of TGF- β or DZ-50 + TGF- β (Fig. 4b).

Anoikis induction was evaluated in LNCaPT β RII and VCaP cells by assessing cell viability on (low adherence) polyHEMA plates. LNCaPT β RII underwent anoikis in response to DZ-50 treatment as observed by the reduced number of live cells 24 h after treatment (Fig. 4c). We did not observe any significant differences in the growth profile of the VCaP cells under various treatment conditions in polyHEMA culture plates. The invasion potential of the LNCaPT β RII and VCaP cells was investigated using the Matrigel

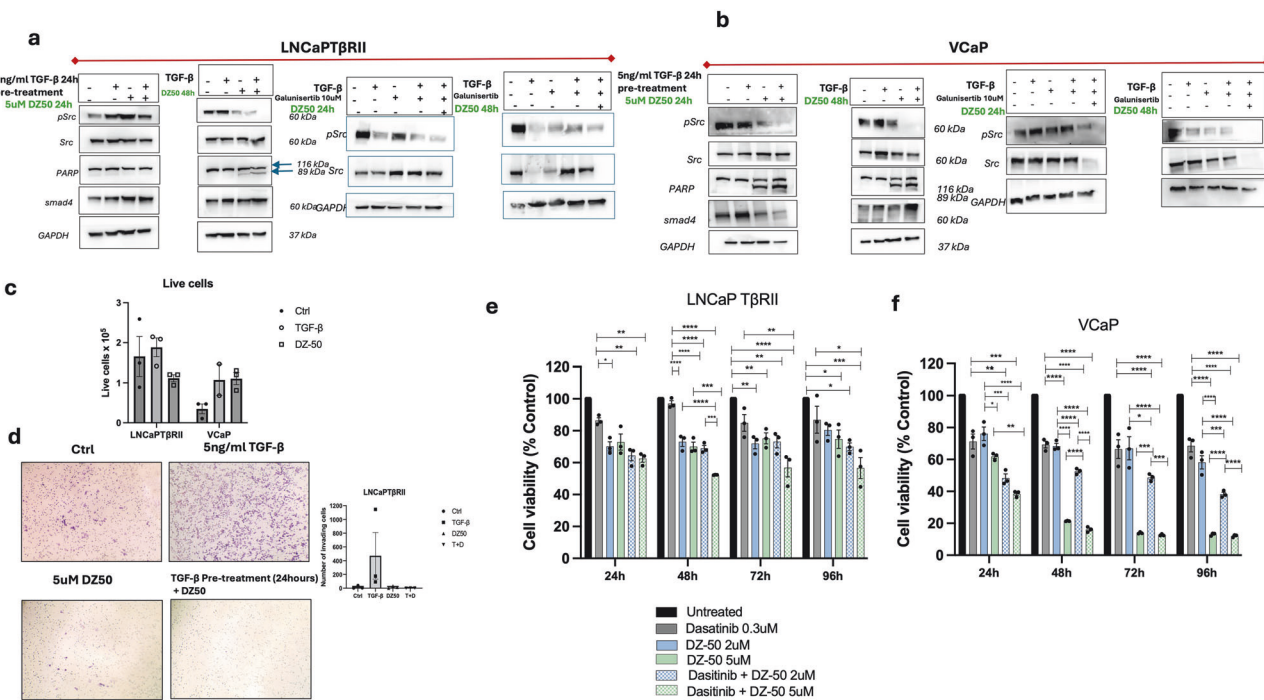


Fig. 4 DZ-50 targets activated Src (survival effector) in LNCaPT β RII and VCaP cells. Western blot analysis of phosphorylated-SRC in **a** LNCaPT β RII and **b** VCaP cells in response to: (i) no treatment, (ii) TGF- β (5 ng/ml), (iii) DZ-50 (5 μ M, 24 or 48 h) or (iv) 24 h pre-treatment with TGF- β followed by DZ-50 (5 μ M, 24 or 48 h). Phosphorylated SRC was also evaluated after TGFBR1 inhibitor-galunisertib treatment (10 μ M) alone or with TGF- β (5 ng/ml) or 24 h pre-treatment with TGF- β and Galunisertib followed by DZ-50 (5 μ M, 24 or 48 h). The data represents three independent experiments. Phosphorylated Src was reduced in response to DZ-50 treatment. **c** Cells were kept in low suspension conditions in polyHEMA treated plates and viability was measured using trypan blue in non-treated and 24 h after TGF- β (5 ng/ml), DZ-50 treatment (5 μ M) in LNCaPT β RII or VCaP cells. **d** Matrigel invasion assay in LNCaPT β RII cells after TGF- β (5 ng/ml), DZ-50 (5 μ M) or TGF- β and DZ-50 treatment. Cell viability assay in **e** LNCaPT β RII cells or **f** VCaP cells in response to Dasatinib (0.3 μ M) or DZ-50 alone (2 or 5 μ M) or co-treatment with dasatinib and DZ-50. Bars \pm SEM $n = 3$ independent experiments. Each experiment was performed in triplicates. * $p < 0.05$, ** $p < 0.01$, *** $p < 0.001$, **** $p < 0.0001$.

invasion assay. Within 48 h, TGF- β increased the cell invasion capacity of LNCaPT β RII cells (Fig. 4d). Treatment of LNCaPT β RII cells with DZ-50 after TGF- β , significantly reduced the number of invading cells (Fig. 4d). On the contrary, there were no changes in the invasion potential of VCaP cells in response to different treatments (Fig. Supplementary 3). As SRC phosphorylation is a marker of anoikis (Fig. 4), we assessed the consequences of pharmacologic inhibition of SRC by dasatinib (0.3 μ M) on DZ-50 induced cell death. Dasatinib had no significant effect on the survival of LNCaPT β RII cells (Fig. 4e), while it led to significantly higher cell death when used in combination with DZ-50 compared to untreated cells or cells treated with dasatinib alone (Fig. 4e). VCaP cells showed sensitivity to anoikis-inducer DZ-50, as well as the SRC inhibitor dasatinib. DZ-50, as a monotherapy or in combination with dasatinib, led to significantly increased cell death compared to either drug alone. (Fig. 4f).

These results highlight the effect of TGF- β -induced EMT in sensitizing LNCaPT β RII cells to DZ-50, suggesting that this anoikis-inducing drug can potentially find therapeutic success in aggressive prostate cancer.

Anoikis is accompanied with downregulation of actin-regulating proteins

As cofilin is a critical effector of TGF- β signaling related to cancer cell migration and metastasis, we assessed its protein levels in our pre-clinical models [18]. DZ-50 treatment for 48 h significantly decreased cofilin expression in LNCaPT β RII cells (Fig. 5a). When these cells were pre-treated with TGF- β (24 h), DZ-50 induced downregulation of cofilin persisted in LNCaPT β RII. Interestingly, when TGF- β activity was blocked with galunisertib, DZ-50 was not able to reduce cofilin in LNCaPT β RII pre-treated with TGF- β , supporting that TGF- β induced

EMT can potentially optimize the response of these cells to DZ-50 induced apoptosis (Fig. 5a). Cofilin in VCaP cells was decreased by DZ-50, while exposure to TGF- β prior to DZ-50 treatment (48 h) led to complete loss of cofilin expression in VCaP cells (Fig. 5a). This effect on cofilin expression was reversed when VCaP cells were treated with galunisertib, TGF- β and DZ-50 (Fig. 5a). As shown in Fig. 5b, the transcriptomic data of protein-protein interactions (PPI) between cofilin and other genes revealed a differential association pattern between LNCaPT β RII and VCaP cells. There was a positive correlation of cofilin with several genes, including WDR, CTTN, ACTG1, ARPC5, ACTB, and PFN1 in LNCaPT β RII. In contrast, in VCaP cells, cofilin positively correlated with WASL, LIMK2, ARPC4, LIMK1, and WHAMM (Fig. 5b and Supplementary Fig. 4).

We observed that in LNCaPT β RII cells anoikis alone (DZ-50 treatment) and EMT preceding anoikis induction (TGF- β pre-treatment followed by DZ-50) led to the activation of a variety of metabolic pathways, such as lipid phosphatase activity, sphingosine metabolic process and membrane lipid biosynthesis (Fig. 6). We also examined genes modulated in response to DZ-50 alone [49] and TGF- β followed by DZ-50 (136) and discovered that 29 genes were commonly regulated between the two processes (Fig. 6). Genes, such as JAM2, PRKCZ-AS1, MAFK1, MARS1, ICMT, and ARHGAP31 were up-regulated in response to DZ-50 alone and TGF- β with DZ-50 compared to untreated and TGF- β treatment.

LNCaPT β RII cells in response to DZ-50 exhibited metabolic changes that were EMT independent.

DZ-50 overcomes therapeutic resistance in prostate cancer cell models

We subsequently evaluated the cell death response of prostate cancer cell lines 22RV1 (CRPC), C42B-Parental or C42B-TaxR (TGF β

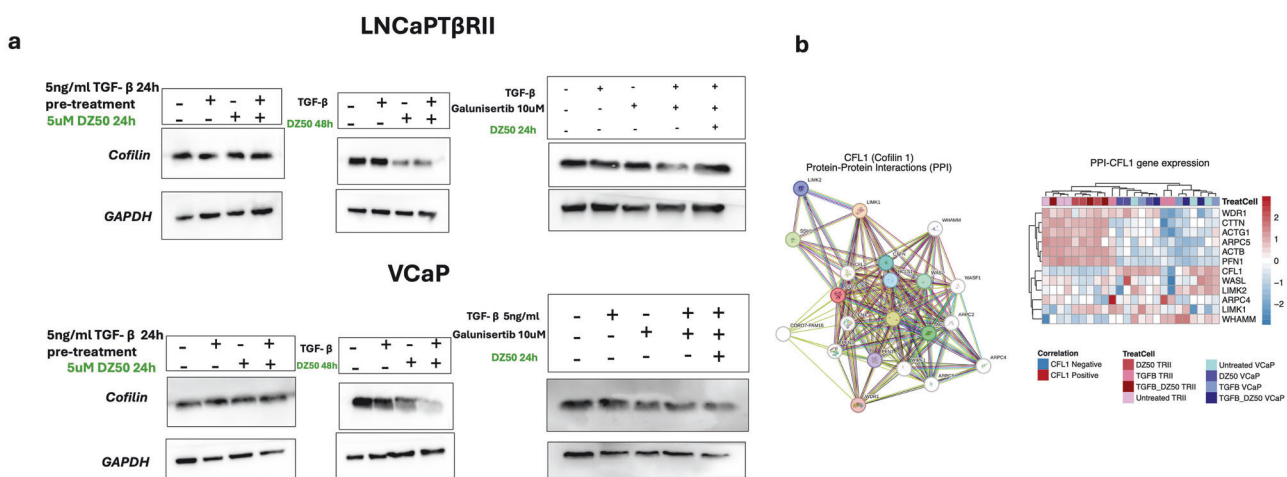


Fig. 5 Anoikis-induction is associated with decreased cofilin in prostate cancer cells. a Protein expression of actin-severing protein Cofilin in LNCaPT β RII cells and VCaP cells after: (i) no treatment, (ii) TGF- β (5 ng/ml), (iii) DZ-50 (5 μ M, 24 or 48 h) or (iv) 24 h pre-treatment with TGF- β followed by DZ-50 (5 μ M, 24 or 48 h). The blots on the right represent LNCaPT β RII cells and VCaP cells receiving: (i) no treatment (ii) Galunisertib (10 μ M) (iii) DZ-50 (5 μ M, 24 or 48 h) (iv) TGF- β (5 ng/ml) and Galunisertib (10 μ M) (v) 24 h pre-treatment with TGF- β and Galunisertib followed by DZ-50 (5 μ M, 24 or 48 h). Data represent three independent experiments. **b** Protein–protein interactions between cofilin and other genes in response to no treatment, DZ-50 alone 9 h, TGF- β 24 h, DZ-50 9 h or pre-treatment with TGF- β for 24 h followed by 9 h of DZ-50.

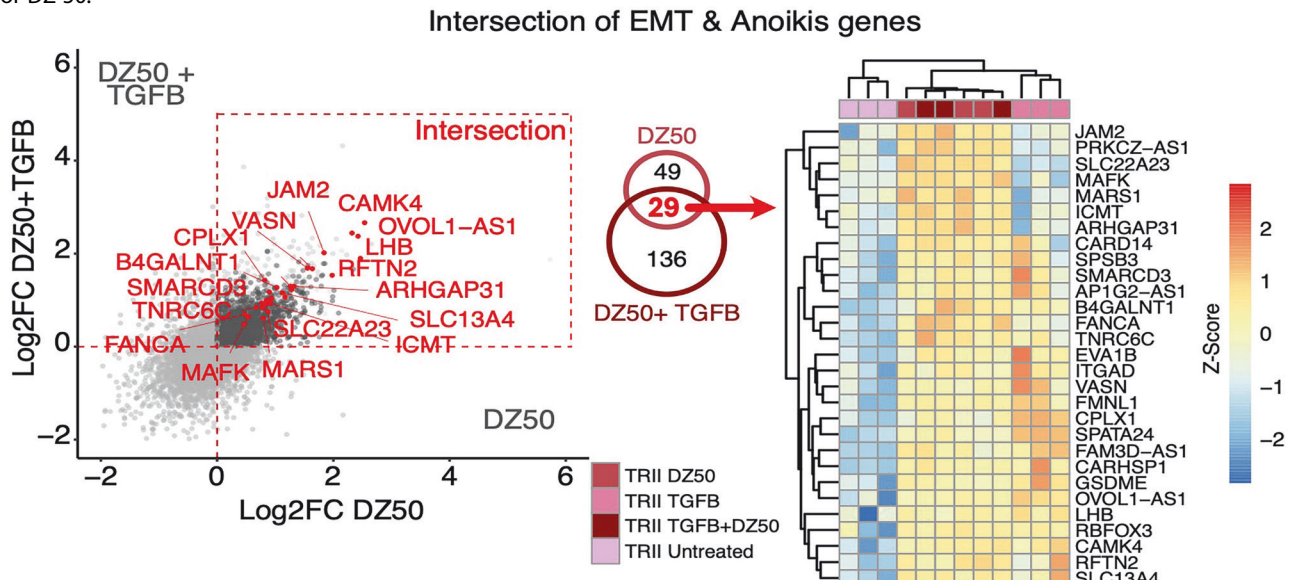


Fig. 6 Metabolic pathways are activated in LNCaPT β RII cells after EMT and anoikis induction. Heat map and pathway analysis showing genes [29] commonly regulated after DZ-50 treatment (9 h) (anoikis) or TGF- β pre-treatment + DZ-50 for 9 h (EMT followed by anoikis). Both anoikis induction alone and phenotypic reprogramming, followed by anoikis, leads to the activation of metabolic pathways in cancer cells.

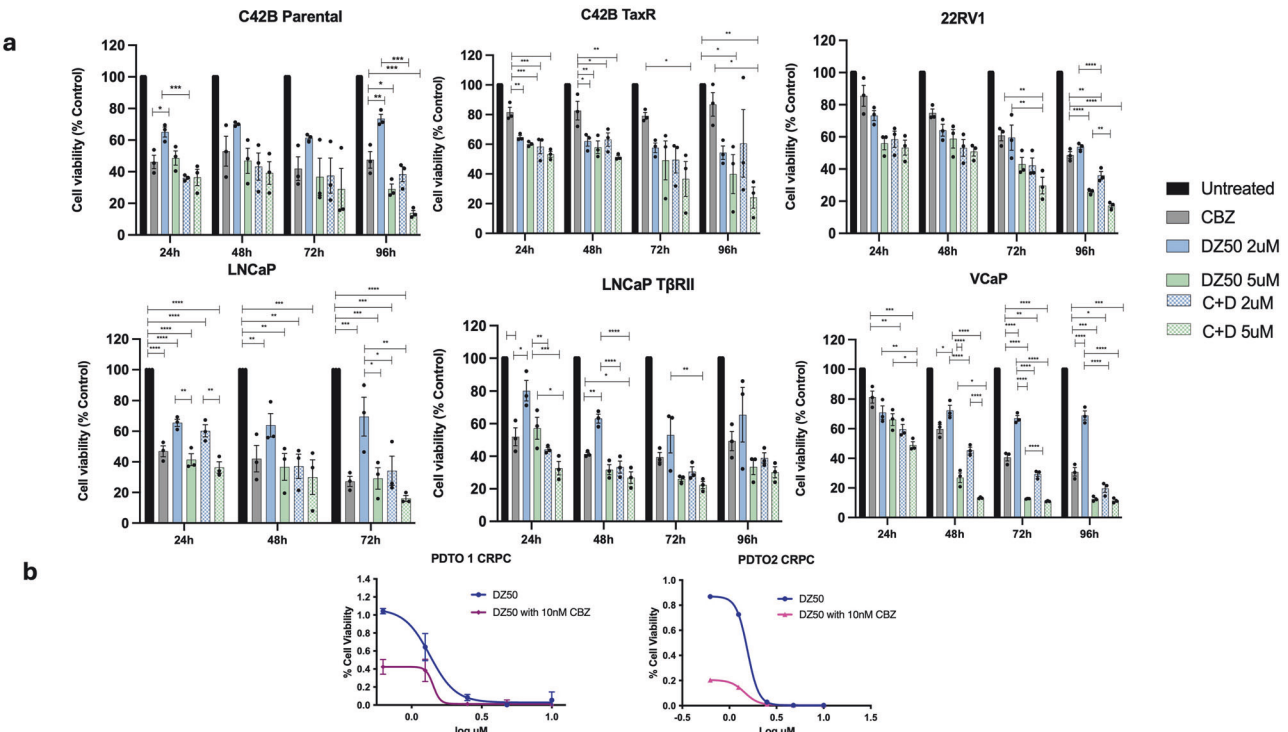


Fig. 7 Anoikis-induction overcomes therapeutic resistance to cabazitaxel in prostate cancer cells. **a** Prostate cancer cell lines were subjected to treatment with CBZ (10 nM) alone or in combination with DZ-50 (2 or 5 μ M) for 24, 48 or 72 h. C42B-TaxR cells that are unresponsive to CBZ die in response to DZ-50. An improved therapeutic response is observed with combination therapy of DZ-50 and CBZ (C + D) in 22RV1, LNCaP, LNCaPT β RII, and C42BTaxR cells. Bars \pm SEM. * P < 0.05, ** P < 0.01 *** P < 0.001, **** P < 0.0001. n = 3 independent experiments. Each experiment was performed in triplicates. **b** Cell viability assessment in CRPC organoids after 72 h treatment with six doses as indicated of DZ-50 alone or CBZ (10 nM) in combination with DZ-50.

unresponsive, taxane resistant), LNCaP (androgen sensitive), LNCaPT β RII (androgen-sensitive; TGF β responsive) or VCaP (androgen-sensitive; TGF- β responsive); to CBZ as a monotherapy or in combination with DZ-50. As shown in Fig. 7, the C42B-Parental cells exhibited a similar response to CBZ, DZ-50 and combination (CBZ + DZ-50) with significant loss of cell viability compared to untreated cells over a treatment time course. C42B-TaxR are resistant to taxane chemotherapy [5]. However, treatment with anoikis-inducing agent DZ-50 significantly decreased cell viability, compared to cell response to CBZ monotherapy. In response to the combination treatment of CBZ and DZ-50, the C42B-TaxR cells exhibited significant loss of survival (Fig. 7a). In the CRPC 22RV1 cells, CBZ alone (10 nM) and DZ-50 alone (2 or 5 μ M) induced significant cell death (72 h). There was an enhanced response by 22RV1 cells to combination treatment compared to CBZ alone (Fig. 7a), suggesting that the anoikis effect can overcome therapeutic resistance. Treatment of LNCaPT β RII and LNCaP cells with DZ-50 and CBZ led to a significant loss of cell viability compared to DZ-50 alone (Fig. 7a). Moreover, there was an increased response anoikis (~10% cell viability after 5 μ M DZ-50 over longer treatment periods 48–96 h) (Fig. 7a).

We next assessed the therapeutic potential of DZ-50 induced anoikis in *in vivo* organoid models derived from patients with CRPC [26] (Fig. 7b). We found that the organoids respond to DZ-50 in a dose-dependent manner (Fig. 7b). While both CRPC organoid models exhibited similar responses to CBZ as a single agent (Supplementary Fig. 5), treatment with CBZ and DZ-50 combination significantly suppressed tumor growth in both models (Fig. 7b).

DISCUSSION

Clinical challenges in diagnosing and treating CRPC are a result of complex tumor cell heterogeneity and the emergence of

treatment resistance [31]. Previous work from our group pursuing apoptosis-inducing therapeutics against CRPC identified that α_1 -adrenoceptor antagonists used to treat benign prostatic hyperplasia exhibit a potent anti-tumor effect [32, 33]. Structural optimization led to the generation of novel compounds (lead agent DZ-50) with a potent anoikis-inducing effect against tumor growth and vascularity [14, 23, 28]. In the present study, we utilize this agent as a tool to leverage therapeutic effectiveness, overcome therapy resistance and identify mechanisms of intersection between anoikis and phenotypic EMT for the treatment of mCRPC (Graphical abstract). DHT inhibits TGF- β -induced caspase-3-driven apoptosis by reducing the expression of TGF- β receptor II [34]. While TGF- β induces a mesenchymal phenotype in LNCaPT β RII cells, which is reversed by DZ-50, the VCaP cells undergo apoptosis in response to TGF- β . Activated SRC is implicated in prostate cancer progression via engaging AR, TGF- β , and ERK signaling [35]. DZ-50 effectively reduced SRC phosphorylation (anoikis) in both LNCaPT β RII and VCaP cells (Graphical abstract).

Anoikis induced by DZ-50 is enhanced in LNCaPT β RII cells when they are primed by TGF- β to undergo phenotypic transition. In the VCaP cells, the apoptotic response to DZ-50 is TGF- β -independent, as evident from the loss of cell viability observed following the combination treatment with galunisertib and DZ-50. Evidence suggests that TGF- β induces an apoptotic response in PC3U (cells from PC3 human prostatic adenocarcinoma cells derived from bone metastases) mediated by Smad7 [36]. We observed decreased protein levels of mesenchymal markers, such as vimentin and snail, in parallel with anoikis induction, suggesting a novel signature of anoikis resistance as a prognostic indicator of prostate cancer outcomes [37].

Anoikis-related gene signatures (CDKN1A, PLK1, TAGLN genes) are recognized as a potential prognostic model for renal papillary cell carcinoma [38]. CDKN1A has been identified as a prognostic

anoikis-related gene, with its upregulation in clear cell renal cell carcinoma and head and neck squamous carcinoma linked to protective effects, while its loss is associated with poor clinical outcomes [39]. In accordance, we found that treatment of VCaP cells with DZ-50 alone or a combination of TGF- β and DZ-50 leads to up-regulation of CDKN1A. Neural precursor cell expressed, developmentally downregulated 9 (NEDD9) belongs to the Crk-associated substrate family of proteins that mediate processes, such as cell cycle and cytoskeletal organization [40], as well as EMT and oncogenic signaling in different cancers [41]. NEDD9 is strongly induced by TGF- β in prostate cancers, wherein its knockdown led to a reduction in TGF- β -associated tumor invasion, and the level of NEDD9 in patient samples was associated with tumor aggressiveness and metastasis [40]. Here we report significant upregulation of NEDD9 in response to TGF- β in LNCaPT β RII cells, and DZ-50 treatment not only reverses this upregulation but also suppresses EMT-genes.

Actin skeletal remodeling is a hallmark of cancer progression and cofilin has been established as an orchestrator of prostate cancer progression and therapeutic resistance [18, 42–44]. Here, we observe that anoikis induction by DZ-50 effectively reduces cofilin expression. Besides transcriptomic analysis demonstrates strong interaction between cofilin (CFL1) and actin (ACTG1) genes in LNCaPT β RII cells. Actin-related protein 2/3 complex subunit 5 (ARPC5) has been validated as a critical regulator of migration and invasion in diverse cancers, including prostate cancer [45, 46]; proliferation was also reduced upon ARPC5 depletion [45]. PPI analysis in our study shows a positive correlation between ARPC5 and cofilin genes in LNCaPT β RII cells. LIM-domain kinase-2 (LIMK2), an actin regulator via cofilin in normal cells and a metastatic and angiogenesis regulator in cancer cells, has been studied to be a clinical target for the prevention and treatment of CRPC because of its upregulation in response to ADT and castration surgery [47, 48]. LIMK1 is associated with increased cell motility and prostate cancer invasiveness [49]. In our studies, VCaP cells had a heightened correlation between LIMK1 and LIMK2 with cofilin.

Junctional adhesion molecule 2 (JAM2) gene encodes a tight junction membrane protein, which is a potential prognostic biomarker that inhibits proliferation, metastasis and EMT in lung adenocarcinoma [50]. Low JAM2 expression is also associated with poor prognosis and survival outcomes in patients [50, 51]. As lipid metabolism leads to changes in the prostate that can drive therapeutic resistance to antiandrogens [52], targeting prostate cancer lipid metabolism, including synthesis, uptake, and oxidation, can provide novel therapeutic platforms [52]. In accordance with this concept, LNCaPT β RII cells in response to DZ-50 exhibited extensive metabolic changes, independently of EMT. Understanding the mechanisms associated with treatment resistance and using targeted therapies to overcome such resistance is critical to combating lethal disease [53, 54].

By acting as an anoikis inducer and promoting phenotypic reprogramming, DZ-50 effectively counters TGF- β -induced EMT towards improving therapeutic response in LNCaPT β RII cells. The current study provides new insights into the intersection of EMT with anoikis, which can be exploited for therapeutic vulnerability in prostate cancer and enabling tailored therapeutic responses for individual tumors.

DATA AVAILABILITY

Data processing and analysis scripts are deposited in GitHub (<https://github.com/eegk/TGF-beta-Prostate-Cancer-Cell-Anoikis-Response>). All other relevant data that support the conclusions of the study are within the supplementary material or available from the authors upon request.

REFERENCES

- Nepali PR, Kyprianou N. Anoikis in phenotypic reprogramming of the prostate tumor microenvironment. *Front Endocrinol*. 2023;14:1160267.
- Siegel RL, Giaquinto AN, Jemal A. Cancer statistics, 2024. *CA Cancer J Clin*. 2024;74:12–49.
- Tan MHE, Li J, Xu HE, Melcher K, Yong E-I. Androgen receptor: structure, role in prostate cancer and drug discovery. *Acta Pharmacol Sin*. 2015;36:3–23.
- Posdziech P, Darr C, Hilser T, Wahl M, Herrmann K, Hadaschik B, et al. Metastatic prostate cancer-a review of current treatment options and promising new approaches. *Cancers (Basel)*. 2023;15:461. <https://doi.org/10.3390/cancers15020461>.
- Archer M, Begemann D, Gonzalez-Kozlova E, Nepali PR, Labanca E, Shepherd P, et al. Kinesin facilitates phenotypic targeting of therapeutic resistance in advanced prostate cancer. *Mol Cancer Res*. 2024;22:730–45. <https://doi.org/10.1158/1541-7786.MCR-23-1047>.
- Mateo J, Carreira S, Sandhu S, Miranda S, Mossop H, Perez-Lopez R, et al. DNA-repair defects and olaparib in metastatic prostate cancer. *N Engl J Med*. 2015;373:1697–708.
- Mateo J, Porta N, Bianchini D, McGovern U, Elliott T, Jones R, et al. Olaparib in patients with metastatic castration-resistant prostate cancer with DNA repair gene aberrations (TOPARP-B): a multicentre, open-label, randomised, phase 2 trial. *Lancet Oncol*. 2020;21:162–74.
- Taylor AK, Kosoff D, Emamekhoo H, Lang JM, Kyriakopoulos CE. PARP inhibitors in metastatic prostate cancer. *Front Oncol*. 2023;13:1159557.
- Huizing MT, Misser VH, Pieters RC, ten Bokkel Huinink WW, Veenhof CH, Vermorken JB, et al. Taxanes: a new class of antitumor agents. *Cancer Investig*. 1995;13:381–404.
- Johnstone RW, Ruefli AA, Lowe SW. Apoptosis: a link between cancer genetics and chemotherapy. *Cell*. 2002;108:153–64.
- Wang J, Ben-David R, Mehrzad R, Yang W, Tewari AK, Kyprianou N. Novel signatures of prostate cancer progression and therapeutic resistance. *Expert Opin Ther Targets*. 2023;27:1195–206.
- Frisch SM, Francis H. Disruption of epithelial cell-matrix interactions induces apoptosis. *J Cell Biol*. 1994;124:619–26.
- Paoli P, Giannoni E, Chiarugi P. Anoikis molecular pathways and its role in cancer progression. *Biochim Biophys Acta*. 2013;1833:3481–98.
- Garrison JB, Shaw YJ, Chen CS, Kyprianou N. Novel quinazoline-based compounds impair prostate tumorigenesis by targeting tumor vascularity. *Cancer Res*. 2007;67:11344–52.
- Hensley PJ, Desinotis A, Wang C, Stromberg A, Chen CS, Kyprianou N. Novel pharmacologic targeting of tight junctions and focal adhesions in prostate cancer cells. *PLoS ONE*. 2014;9:e86238.
- Hensley PJ, Cao Z, Pu H, Dicken H, He D, Zhou Z, et al. Predictive and targeting value of IGFBP-3 in therapeutically resistant prostate cancer. *Am J Clin Exp Urol*. 2019;7:188–202.
- Cao Z, Koochekpour S, Strup SE, Kyprianou N. Reversion of epithelial-mesenchymal transition by a novel agent DZ-50 via IGF binding protein-3 in prostate cancer cells. *Oncotarget*. 2017;8:78507–19.
- Collazo J, Zhu B, Larkin S, Martin SK, Pu H, Horbinski C, et al. Cofilin drives cell-invasive and metastatic responses to TGF- β in prostate cancer. *Cancer Res*. 2014;74:2362–73.
- Martin SK, Pu H, Pentecuff JC, Cao Z, Horbinski C, Kyprianou N. Multinucleation and mesenchymal-to-epithelial transition alleviate resistance to combined cabazitaxel and antiandrogen therapy in advanced prostate cancer. *Cancer Res*. 2016;76:912–26.
- Zhu Y, Liu C, Nadiminty N, Lou W, Tummala R, Evans CP, et al. Inhibition of ABCB1 expression overcomes acquired docetaxel resistance in prostate cancer. *Mol Cancer Ther*. 2013;12:1829–36.
- Wu H-C, Hsieh J-T, Gleave ME, Brown NM, Pathak S, Chung LWK. Derivation of androgen-independent human LNCaP prostatic cancer cell sublines: role of bone stromal cells. *Int J Cancer*. 1994;57:406–12.
- Guo Y, Kyprianou N. Overexpression of transforming growth factor (TGF) beta1 type II receptor restores TGF-beta1 sensitivity and signaling in human prostate cancer cells. *Cell Growth Differ*. 1998;9:185–93.
- Sakamoto S, McCann RO, Dhir R, Kyprianou N. Talin1 promotes tumor invasion and metastasis via focal adhesion signaling and anoikis resistance. *Cancer Res*. 2010;70:1885–95.
- Bretland AJ, Lawry J, Sharrard RM. A study of death by anoikis in cultured epithelial cells. *Cell Prolif*. 2001;34:199–210.
- Pauli C, Hopkins BD, Prandi D, Shaw R, Fedrizzi T, Sboner A, et al. Personalized in vitro and in vivo cancer models to guide precision medicine. *Cancer Discov*. 2017;7:462–77.
- Puca L, Bareja R, Prandi D, Shaw R, Benelli M, Karthaus WR, et al. Patient derived organoids to model rare prostate cancer phenotypes. *Nat Commun*. 2018;9:2404.
- Cao Z, Kyprianou N. Mechanisms navigating the TGF- β pathway in prostate cancer. *Asian J Urol*. 2015;2:11–8.
- Sakamoto S, Kyprianou N. Targeting anoikis resistance in prostate cancer metastasis. *Mol Asp Med*. 2010;31:205–14.
- Kaufmann SH, Desnoyers S, Ottaviano Y, Davidson NE, Poirier GG. Specific proteolytic cleavage of poly(ADP-ribose) polymerase: an early marker of chemotherapy-induced apoptosis1. *Cancer Res*. 1993;53:3976–85.

30. Pu H, Horbinski C, Hensley PJ, Matuszak EA, Atkinson T, Kyprianou N. PARP-1 regulates epithelial-mesenchymal transition (EMT) in prostate tumorigenesis. *Carcinogenesis*. 2014;35:2592–601.
31. Livas L, Hasani S, Kyprianou N. Integrated therapeutic targeting of the prostate tumor microenvironment. *Adv Exp Med Biol*. 2020;1296:183–98.
32. Chon JK, Borkowski A, Partin AW, Isaacs JT, Jacobs SC, Kyprianou N. Alpha 1-adrenoceptor antagonists terazosin and doxazosin induce prostate apoptosis without affecting cell proliferation in patients with benign prostatic hyperplasia. *J Urol*. 1999;161:2002–8.
33. Kyprianou N. Doxazosin and terazosin suppress prostate growth by inducing apoptosis: clinical significance. *J Urol*. 2003;169:1520–5.
34. Song K, Wang H, Krebs TL, Kim SJ, Danielpour D. Androgenic control of transforming growth factor-beta signaling in prostate epithelial cells through transcriptional suppression of transforming growth factor-beta receptor II. *Cancer Res*. 2008;68:8173–82.
35. Vlaeminck-Guillem V, Gillet G, Rimokh R. Src: marker or actor in prostate cancer aggressiveness. *Front Oncol*. 2014;4:222. <https://doi.org/10.3389/fonc.2014.00222>.
36. Edlund S, Bu S, Schuster N, Aspenström P, Heuchel R, Heldin NE, et al. Transforming growth factor-beta1 (TGF-beta)-induced apoptosis of prostate cancer cells involves Smad7-dependent activation of p38 by TGF-beta-activated kinase 1 and mitogen-activated protein kinase kinase 3. *Mol Biol Cell*. 2003;14:529–44.
37. Chen K, Zhang Y, Li C, Liu Y, Cao Q, Zhang X. Clinical value of molecular subtypes identification based on anoikis-related lncRNAs in castration-resistant prostate cancer. *Cell Signal*. 2024;117:111104.
38. Gan L, Xiao Q, Zhou Y, Fu Y, Tang M. Role of anoikis-related gene PLK1 in kidney renal papillary cell carcinoma: a bioinformatics analysis and preliminary verification on promoting proliferation and migration. *Front Pharmacol*. 2023;14:1211675. <https://doi.org/10.3389/fphar.2023.1211675>.
39. Li J, Cao Q, Tong M. Deciphering anoikis resistance and identifying prognostic biomarkers in clear cell renal cell carcinoma epithelial cells. *Sci Rep*. 2024;14:12044.
40. Morimoto K, Tanaka T, Nitta Y, Ohnishi K, Kawashima H, Nakatani T. NEDD9 crucially regulates TGF-β-triggered epithelial-mesenchymal transition and cell invasion in prostate cancer cells: Involvement in cancer aggressiveness. *Prostate*. 2014;74:901–10.
41. Gabbasov R, Xiao F, Howe CG, Bickel LE, O'Brien SW, Benrubi D, et al. NEDD9 promotes oncogenic signaling, a stem/mesenchymal gene signature, and aggressive ovarian cancer growth in mice. *Oncogene*. 2018;37:4854–70.
42. Chen L, Cai J, Huang Y, Tan X, Guo Q, Lin X, et al. Identification of cofilin-1 as a novel mediator for the metastatic potentials and chemoresistance of the prostate cancer cells. *Eur J Pharmacol*. 2020;880:173100.
43. Martin SK, Kamelgarn M, Kyprianou N. Cytoskeleton targeting value in prostate cancer treatment. *Am J Clin Exp Urol*. 2014;2:15–26.
44. Fu F, Yu Y, Zou B, Long Y, Wu L, Yin J, et al. Role of actin-binding proteins in prostate cancer. *Front Cell Dev Biol*. 2024;12:1430386. <https://doi.org/10.3389/fcell.2024.1430386>.
45. Qu G, Zhang Y, Duan H, Tang C, Yang G, Chen D, et al. ARPC5 is transcriptionally activated by KLF4, and promotes cell migration and invasion in prostate cancer via up-regulating ADAM17 : ARPC5 serves as an oncogene in prostate cancer. *Apoptosis*. 2023;28:783–95.
46. Ming Y, Luo C, Ji B, Cheng J. ARPC5 acts as a potential prognostic biomarker that is associated with cell proliferation, migration and immune infiltrate in gliomas. *BMC Cancer*. 2023;23:937.
47. Nikhil K, Chang L, Viccaro K, Jacobsen M, McGuire C, Satapathy SR, et al. Identification of LIMK2 as a therapeutic target in castration resistant prostate cancer. *Cancer Lett*. 2019;448:182–96.
48. Sumi T, Matsumoto K, Takai Y, Nakamura T. Cofilin phosphorylation and actin cytoskeletal dynamics regulated by rho- and Cdc42-activated LIM-kinase 2. *J Cell Biol*. 1999;147:1519–32.
49. Ahmed T, Shea K, Masters JRW, Jones GE, Wells CM. A PAK4-LIMK1 pathway drives prostate cancer cell migration downstream of HGF. *Cell Signal*. 2008;20:1320–8.
50. Dong Y, Zhang J, Xie S, Di S, Fan B, Gong T. JAM2 is a prognostic biomarker and inhibits proliferation, metastasis and epithelial-mesenchymal transition in lung adenocarcinoma. *J Gene Med*. 2024;26:e3679.
51. Peng Y, Li H, Fu Y, Guo S, Qu C, Zhang Y, et al. JAM2 predicts a good prognosis and inhibits invasion and migration by suppressing EMT pathway in breast cancer. *Int Immunopharmacol*. 2022;103:108430.
52. Stoykova GE, Schlaepfer IR. Lipid metabolism and endocrine resistance in prostate cancer, and new opportunities for therapy. *Int J Mol Sci*. 2019;20:2626. <https://doi.org/10.3390/ijms20112626>.
53. Haldrup J, Weiss S, Schmidt L, Sørensen KD. Investigation of enzalutamide, docetaxel, and cabazitaxel resistance in the castration resistant prostate cancer cell line C4 using genome-wide CRISPR/Cas9 screening. *Sci Rep*. 2023;13:9043. <https://doi.org/10.1038/s41598-023-34442-1>.
54. Hongo H, Kosaka T, Suzuki Y, Oya M. Discovery of a new candidate drug to overcome cabazitaxel-resistant gene signature in castration-resistant prostate cancer by *in silico* screening. *Prostate Cancer Prostatic Dis*. 2023;26:59–66.

AUTHOR CONTRIBUTIONS

PR Nepali: conceptualization of research study, investigation, designing and conducting experiments, acquiring and analyzing data, writing and editing of manuscript. E Gonzalez-Kozlova: investigation, data acquisition, data analysis and representation, methodology, reviewing of manuscript. M Anegondi: designing and conducting experiments, data acquisition and analysis. N Dogra: data discussion, data acquisition, manuscript review. M Archer: experimental design, methodology and manuscript review. G Chakraborty: experimental conceptualization, methodology and investigation, data discussion, funding acquisition. AK Tewari: manuscript review and funding acquisition. BD Hopkins: designing and conducting experiments, data acquisition and analysis, manuscript review. N Kyprianou: conceptualization of research study, investigational design, methodology, resources, project supervision, funding acquisition, writing, reviewing and editing of manuscript.

FUNDING

This work was supported by: Natasha Kyprianou: National Institutes of Health/NCI Grant number R01 CA232574. Edgar Gonzalez-Kozlova: NCI-NIH-U24CA224319. Navneet Dogra: National Institutes of Health Grant number R21 AGO78848. Goutam Chakraborty: National Institute of Health (NCI) Grant number R01 R01CA274967, Department of Defense (W81XWH-19-1-0470), Prostate Cancer Foundation Young Investigator Award and NYS Prostate Cancer Pilot Project Award; TCI Scholars Award.

COMPETING INTERESTS

NK serves on the advisory board for Onconox Inc. GC has served as a scientific consultant for GuidePoint and GLG and received consultation fees. AKT has served as a site-PI on sponsored clinical trials from Kite Pharma Inc., Lumicell Inc., Dendron Pharmaceuticals, LLC, Oncovir Inc., Blue Earth Diagnostics Ltd, RhoVac ApS, Bayer HealthCare Pharmaceuticals Inc. and Janssen Research and Development, LLC. The other authors declare no competing interests.

ETHICS APPROVAL AND CONSENT TO PARTICIPATE STATEMENT

All experiments have been performed in accordance with the relevant guidelines and regulations. This research article does not include any studies with live vertebrates or humans.

ADDITIONAL INFORMATION

Supplementary information The online version contains supplementary material available at <https://doi.org/10.1038/s41388-025-03600-z>.

Correspondence and requests for materials should be addressed to Natasha Kyprianou.

Reprints and permission information is available at <http://www.nature.com/reprints>

Publisher's note Springer Nature remains neutral with regard to jurisdictional claims in published maps and institutional affiliations.



Open Access This article is licensed under a Creative Commons Attribution-NonCommercial-NoDerivatives 4.0 International License, which permits any non-commercial use, sharing, distribution and reproduction in any medium or format, as long as you give appropriate credit to the original author(s) and the source, provide a link to the Creative Commons licence, and indicate if you modified the licensed material. You do not have permission under this licence to share adapted material derived from this article or parts of it. The images or other third party material in this article are included in the article's Creative Commons licence, unless indicated otherwise in a credit line to the material. If material is not included in the article's Creative Commons licence and your intended use is not permitted by statutory regulation or exceeds the permitted use, you will need to obtain permission directly from the copyright holder. To view a copy of this licence, visit <http://creativecommons.org/licenses/by-nc-nd/4.0/>.